Investigations of long pulse sodium laser guide stars

Rachel Rampy[a], Donald Gavel[a], Simon Rochester[b], Ronald Holzlöhner[c]
[a]University of California, 1156 High St., Santa Cruz, CA, USA 95064-1099; [b]Rochester Scientific, LLC, 2041 Tapscott Ave., El Cerrito, CA 94530, USA; [c]European Southern Observatory (ESO), Garching bei München, D-85748, Germany

ABSTRACT

Long pulse length sodium laser guide stars (LGS) are useful because they allow for Rayleigh blanking and fratricide avoidance in multiple LGS systems. Bloch equation simulations of sodium-light interactions in Mathematica show that certain spectral formats and pulse lengths, on the order of 30 microseconds, with high duty cycles (20–50%) should be able to achieve photon returns within 10% of what is seen from continuous wave (CW) excitation. In this work, we investigate the time dependent characteristics of sodium fluorescence, and find the optimal format for the new LGS that will be part of the upgraded AO system on the Shane 3 Meter telescope at Mt. Hamilton. Results of this analysis are discussed along with their general applicability to other LGS systems. The potential benefits of uplink correction are also considered.

Keywords: laser guide stars, sodium florescence, Shane AO, uplink correction

1. INTRODUCTION

Use of laser guide stars (LGS) along with adaptive optics (AO) allows large telescopes to significantly improve resolution by correcting image distortion induced by atmospheric turbulence. LGS enable creation of the beacon used to measure the distortion at different locations in the sky. This is necessary for AO observations of astronomical targets that lack nearby natural guide stars (NGS). Sodium (Na) LGS operating at a wavelength of 589 nm are preferable due to the high altitude of the sodium layer in Earth's mesosphere (around 80–100km), fluorescence at visible wavelengths, and a large fluorescence cross section-abundance product compared to the other constituents of the upper atmosphere. The idea of Na LGS was first proposed in the 1980's, began to be realized in the 1990's[1,2], and future adaptive telescopes will require them in nearly all science operations.

Because powerful diffraction-limited laser beams at 589 nm are expensive to produce, careful optimization of the laser format (spectrum, polarization, spot size) is necessary. Numerical models allow us to investigate the various physical mechanisms occurring in the laser-Na system that affect the number of photons returned to the telescope. Results presented here were obtained using a density-matrix calculation with coupled velocity groups, and included the important physical effects of Larmor precession due to the geomagnetic field, radiation pressure (recoil), saturation, velocity-changing and spin-randomizing collisions[3]. The LGSBloch package is run in Mathematica, and based on the Atomic Density Matrix package written by S. Rochester[4].

Motivation for this research is provided by the near future upgrade of the AO system on the 3 meter Shane Telescope at Lick Observatory. The Shane hosted the first experiments in Na LGS AO, with observations starting in 1996, and provides for regular astronomical science observing to this day. The new system will incorporate many of the recent advancements in AO technology and lessons learned from laboratory and on-sky experiments in order to provide higher Strehl, improved sensitivity, and greater wavelength coverage for astronomers. This second generation system uses a 32x32 actuator MEMS deformable mirror, with a higher sensitivity wavefront sensor, and new fiber laser developed at Lawrence Livermore National Laboratory (LLNL). Aside from the practical advantages of being more compact and using much less power than the dye laser currently in use, the fiber laser allows us to adjust the pulse and spectral format for optimal coupling to the mesospheric sodium atoms. The goal of this investigation is to ascertain the ideal values of these parameters, and to estimate the return signal.

In section 2, details of the relevant sodium physics pertaining to the numerical model are given, followed by discussion of the suggested optimal format and projected return flux for the new LGS in section 3. Section 4 presents a comparison

between modeling calculations and data from the current LGS systems at the Lick and Keck Observatories, and section 5 discusses what the results of this investigation suggest for other systems, and addresses the potential benefits of uplink correction.

2. NUMERICAL SIMULATIONS OF LGS

Sodium LGS take advantage of the $3^2S_{1/2} - 3^2P_{3/2}$ dipole transition, known as the D_2 line. The sodium ground state consists of two hyperfine multiplets with 8 magnetic substates combined. The hyperfine states are separated by 1.77 GHz, splitting the D_2 line into the D_2a and D_2b transition groups. These correspond respectively to the $F = 1$ and $F = 2$ ground states, where F is the total atomic angular momentum quantum number. The four excited state multiplets ($F = 0$, …,3) are separated by only 16, 34, and 60 MHz, and contain a total of 16 magnetic substates. At mesospheric temperatures of about 190 K, the D_2a and D_2b lines are Doppler broadened to ~1 GHz each, giving rise to the characteristic double-hump absorption profile shown in Figure 1 (we note that this profile is only valid at very low irradiance levels far below those typical for LGS in the mesosphere; at higher irradiance levels, the profile becomes dependent on several factors such as laser polarization and the geomagnetic field).

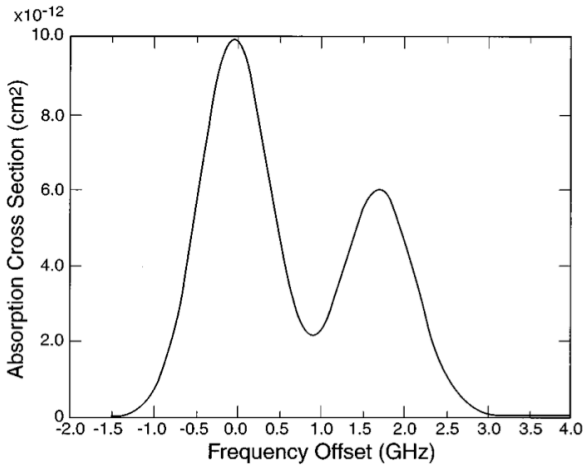

Figure 1. The absorption profile of the D_2 line in sodium has two distinct peaks due to the 1.77 GHz splitting between the hyperfine levels of the ground state. These are referred to as D_2a and D_2b and are shown here with Doppler broadening characteristic of mesospheric temperatures around 185 K (credit: Milonni 1998).

Based on theoretical and experimental considerations, maximizing the number of photons emitted back towards the telescope involves use of a circularly polarized beam centered on the D_2a line, with ~10% of the light tuned to the D_2b transition[3,5]. Without this "repumping" 3/8 of atoms in thermal equilibrium would not interact with the laser light, and those that later decayed into the $F = 1$ ground state would be lost. The optical pumping with repumping strategy allows the most atoms to become trapped cycling between the $F = 2$, $m = 2$ ground state and the $F' = 3$, $m = 3$ excited state. The benefits are that this is the strongest transition of the D_2 group, atoms are forbidden by selection rules from decaying to the $F = 1$ ground state, and the florescence is preferentially directed along the light beam (dipole transition).

Several factors reduce the efficiency of optical pumping, including Larmor precession due to the geomagnetic field, collisions with other constituents of the upper atmosphere, and transition saturation leading to stimulated emission (photons are emitted along the laser propagation direction instead of towards the telescope). Also important to consider is the slight change in velocity incurred from absorption and spontaneous emission of a photon (equivalent to a Doppler shift of ~50 kHz, known as atomic recoil), and the transit of Na atoms in and out of the light beam. At the location of Mt. Hamilton the strength of the geomagnetic field is 0.47 Gauss, corresponding to a Larmor precession period of ~3.0 μs. The time between collisions is on the order of ~100 μs, and the atoms in the beam are exchanged on a timescale of several milliseconds. Thus different factors will dominate depending on the duration of the laser pulse.

The quantity of returned photons also depends on the amount of atmospheric absorption, the column density of sodium atoms in the mesosphere, and varies as T_a^{2X}/X, where T_a is the one-way atmospheric transmission at 589 nm at zenith,

and $X = 1/\cos(\zeta)$ is the airmass with the zenith angle ζ. The relative direction of the local geomagnetic field with respect to the laser beam has significant impact, which is maximal when they are perpendicular. Hence, highest returns are achieved when the laser propagates parallel to the field lines. There is also seasonal variation in the Na column density by a factor of ~3, with the high around November and low near May in the northern hemisphere.

To calculate the observed fluorescence, the evolution of the atoms is modeled using the optical Bloch equations for the atomic density matrix, which describes the statistical state of the ensemble of atoms. To account for atoms with different Doppler shifts, the velocity dependence of the density matrix is discretized to describe an appropriate number, $n_{v.g.}$, of velocity groups each with a fixed velocity along the laser beam propagation direction. Because coherences between atoms with different velocities can be neglected, the complete density matrix can be thought of as a collection of $n_{v.g.}$ separate but coupled density matrices, each of dimension 24 × 24. The system is solved using methods built in to Mathematica, and the fluorescent photon flux per solid angle emitted in a given direction is found from the steady-state solution as the expectation value of a fluorescence operator[3,6].

To account for a non-uniform irradiance pattern in the mesosphere, LGSBloch makes use of a Gaussian intensity distribution, with user defined FWHM and number of different irradiance levels to include. Based on experimentation, results do not change significantly when greater than 5 levels are modeled, so this number is used throughout this work. In calculating the return at the telescope, the fluorescing atoms are assumed to be at the median altitude of the Na layer near 92 km. We also adopted an assumed Na column density of 4 x10^{13} atoms/m^2, and 0.5 m FWHM mesospheric spot size, for simulation results presented in the next section.

3. OPTIMIZATION OF PULSED LGS RETURN

The current LGS in use on the Shane Telescope at Lick Observatory is a tuned dye laser, which was constructed at LLNL and installed in 1995. The average measured output power between 2006 and 2010 was 9 Watts. The light is linearly polarized, and contains pulses of 150 ns in duration with a repetition frequency of 11 kHz. The beam is centered on the D_2a line, and electro-optically phase modulated to broaden it to ~2 GHz line width. This was done to address all atoms in the Doppler broadened absorption profile, and attempt to reduce saturation effects due to the high peak power during the pulses. Measurements show this laser gives the equivalent of about a 10th magnitude natural guidestar, which is adequate to run the AO system with its present 43 cm diameter subapertures (i.e. sufficient for $\lambda = 2.0$ μm science observing)[7].

Much has been learned since this laser was installed, both in terms of laser technology and understanding the coupling of laser light to the Na atoms in the mesosphere. In particular, demonstrations of narrow band CW Na LGS have shown a much greater number of returned photons per watt than from the modulated dye lasers[8]. Increasing the return signal will enable use of smaller subapertures, so AO correction can be applied at shorter science wavelengths. Recently LLNL has been involved in developing fiber laser technology for LGS. They have demonstrated a solid state 589 nm system with 10 Watts output power in the lab[9]. It uses non-linear combining of two high-power infrared lasers at 938 nm and 1538 nm to produce the 589 nm line, and has tunable temporal and spectral characteristics. Table 1 gives the parameters of both lasers and shows the current lab tested versus target formats for the fiber laser system.

Table 1: Comparison of parameters between the current LGS and new fiber laser.

	Current dye laser	**New fiber laser**	
		Lab tested format	*Goal format*
Output power	9 W	10 W	10 W
Polarization	Linear	Circular	Circular
Spectral format	~2 GHz FWHM bandwidth	9 lines with 200 MHz spacing	Fewer lines and/or smaller spacing
Pulse duration	150 ns	200 ns	30 μs
Duty cycle	0.16 %	10 %	20 %
Fraction of light tuned to D2b	None	None	10%

The effort to determine the optimal pulse duration began with examining how the number of spontaneously emitted photons varied as a function of time. Figure 2 shows results of two 100 μs simulations for zenith pointing at Mt. Hamilton, with the irradiance levels set to be equal to what is present for 10 Watts launched power operating at a 20% duty cycle. On the left, all the light is on the D_2a transition, and the right plot is for ~10% of the light tuned to D_2b. For both cases there is an initial enhancement in the specific return (i.e. photons/s/sr/atom/(W/m^2) in the mesosphere, a measure of local return flux per laser irradiance[3]), but for the case of no repumping the decline begins sooner, for all but the lowest irradiance levels, and the peaks are considerably lower. These results suggest that for 10 Watts launched power and 20% duty cycle the most efficient use of the Na atoms will be with repumping and pulse durations between 10 – 20 μs. However, if partitioning of the laser light to include the D_2b line is not possible due to engineering constraints, somewhat shorter pulses will likely be favorable.

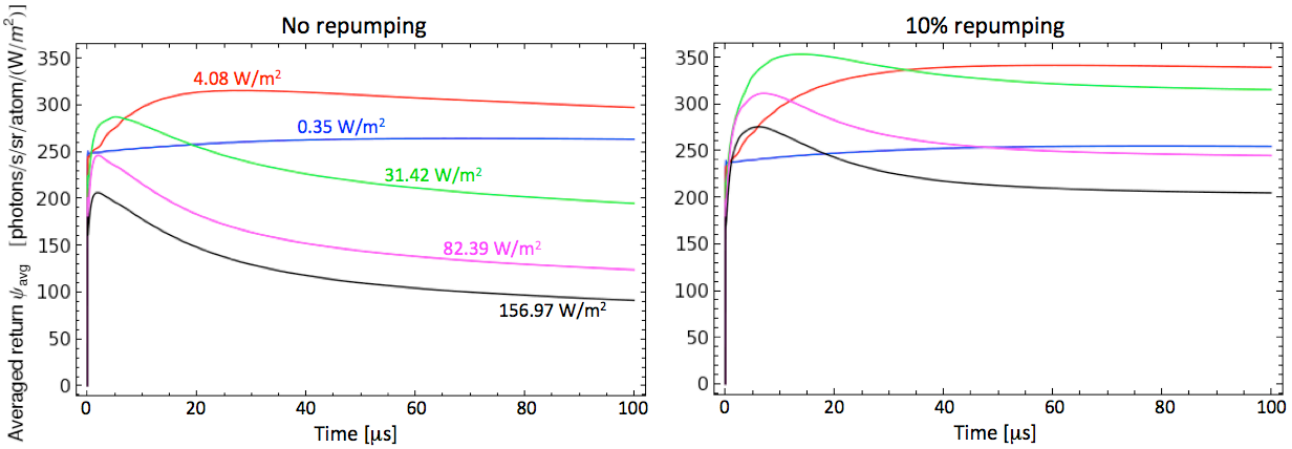

Figure 2. These 100 μs simulations show time evolution of specific return flux for the different levels of irradiance present for 10 Watts launched power with 20% duty cycle. When no light is resonant with the D_2b line (left plot) the return peaks and declines quickly. When 10% of the laser power is tuned to D_2b the return peaks later, is higher, and decreases less rapidly (right plot). These also indicate that certain values of irradiance excite the Na atoms more efficiently.

We hypothesized that the decline after the peak was possibly in part due to the effects of Larmor precession, since it acts on timescales of a few microseconds. To test this, these simulations were repeated with zero magnetic field. The results showed a decrease in the severity of the decline and the expected increase in return, but the peak remained very prominent. This leads to the conclusion that other factors are of greater importance here, such as the rate at which atoms are decaying into the $F = 1$ ground state.

Another interesting result is that certain irradiance levels are more efficient than others. In the above plot for 10% repumping the green line corresponding to 31.42 W/m^2 achieves the highest specific return. The possibility of taking advantage of this circumstance by controlling the irradiance profile using uplink correction will be discussed further in the last section.

Beyond the considerations of how to most effectively excite the sparse Na atoms during a single pulse is the question of what pulse formats allow for the benefits of optical pumping between consecutive pulses. Stated differently, what is the length of time necessary for atomic polarizations to return to thermal equilibrium? Based on results of various simulations this time scale appears to be ~50 μs near the center of the sodium layer. Hence, a format with less then this amount of dark time between pulses should be modeled with multiple cycles of the laser, while pulses with larger spacing may be considered independent, i.e., modeling a single pulse is sufficient. Figure 3 shows a 10 pulse train for pulses of 500 ns, at a 20% duty cycle. It is interesting to note that the different irradiance levels (which are the same as in Figure 2) evolve differently. The extremal levels remain fairly constant from pulse to pulse, while the median values dominate after just a few cycles.

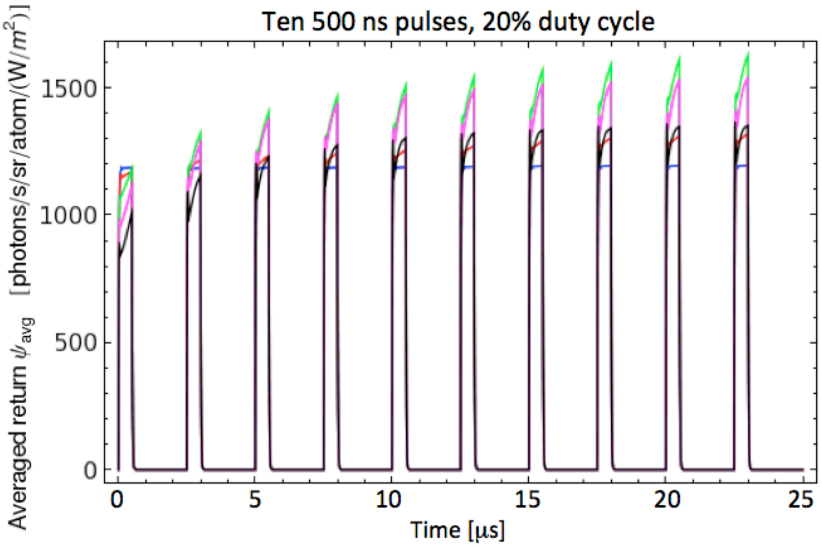

Figure 3. This intermediate pulse format shows the presence of optical pumping between pulses. The irradiance levels and colors are the same as in Figure 2. Again, some levels are more effective than others in this process.

To quantify the benefits of changing the pulse duration, simulations were also carried out for pulses of 500 ns, and 1, 10, 20, 30, 40, and 60 μs. The maximum time-averaged return was found to be for the 30 μs pulse, which has a predicted flux at the telescope of 12 x10^6 photons/s/m^2. This was concluded, based on simulation of 3 cycles of the laser, although it is the same value given for one cycle. At a pulse length of 60 μs the time-averaged return flux declined to 11.3 x10^6 photons/s/m^2. The current pulse length of 200 ns has a predicted flux of 11.4 x10^6 photons/s/m^2 from a simulation of 50 cycles of the laser. For comparison, a 10 Watt CW laser with otherwise all the same parameters is expected to produce 13 x10^6 photons/s/m^2.

The 30 μs pulse has been established as part of the goal format since it will facilitate Raleigh blanking. Based on our modeling the return is also predicted to be ~5% greater than for the lab tested format. Figure 4 contains a time vs. altitude diagram showing how Raleigh blanking can be realized with this pulse format, while having two light pulses in the air at once. Blanking reduces the amount of Raleigh scattered light entering the wavefront sensor measurements, resulting in greater signal-to-noise and increased overall performance of the AO system.

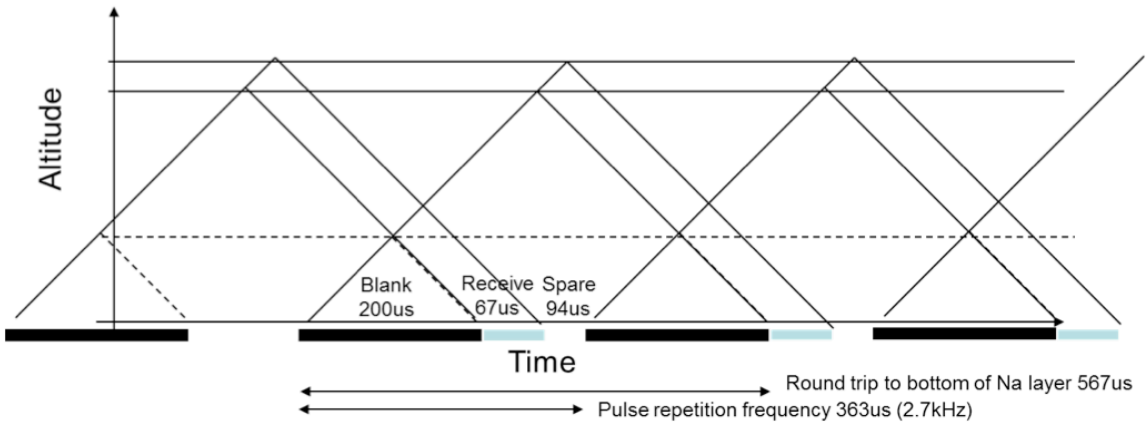

Figure 4. This time vs. altitude diagram demonstrates a Raleigh blanking scheme with two 30 μs pulses in the air at a time.

Our simulation results indicate the optimal format for the new fiber laser should include 10% repumping, and extension of the duty cycle to 20%. For the case of 10% duty cycle and all other parameters the same, the 200 ns pulses are

predicted to return 9.5 x10^6 photons/s/m^2, and the 30 μs pulses 10.1 x10^6 photons/s/m^2. What has not yet been discussed is the broader spectral format of this laser, which currently contains 9 lines spaced at 200 MHz intervals. This format was implemented to mitigate stimulated Brillouin effects (SBS) in the fiber amplifiers. From the standpoint of effective coupling to the Na atoms, this is less desirable than having the light confined within 2 lines tuned precisely to the D_2a and D_2b transitions. Also, the problem of accurately modeling such a system using Bloch equations remains a future research effort due to its complexity. Hence, the return flux numbers presented should be considered optimistic upper limits on what will actually be achievable with this laser in real on-sky conditions.

The average measured return flux from the current dye laser on the Shane telescope between 2006 and 2010 was 1.13 x10^6 photons/s/m^2. Based on modeling of the new fiber laser's return we expect it is reasonable to assume that we will achieve somewhere between 5 and 10 times the current brightness.

4. COMPARISON TO DATA

The LGSBloch simulation package has been confirmed to accurately predict measurements from CW LGS, however, no comparisons have yet been published for pulsed systems. Here we assess how well this method is able to reproduce measurements from the existing LGS systems at the Lick and Keck observatories. The Keck II laser has nearly identical parameters to the Shane LGS, but with a 26 kHz repetition rate and an average of 13 Watts launched power. Measurements reported in the literature indicate between ~0.7 and 1.75 x10^6 photons/s/m^2 are being received at the telescope[10].

Return flux measurements of the Shane LGS are based on data from the Shack-Hartman WFS for zenith pointing observations. The intensity in the fully illuminated subapatures was averaged, and corrected for 40% throughput. The camera gain is reported to be ~1 electron/count. In 2004, D. Gavel used a handheld power meter with 633 nm wavelength light to measure throughput of the AO system from the primary focus of the telescope to the WFS, and found it to be 55%. In January 2012, observations of several Hayes spectrophotometric standard stars were taken to re-asses this value. A sodium filter with 0.87 nm FWHM bandpass was used, and resulting flux measurements were corrected for atmospheric transmission and compared with online spectra[11]. This analysis returned an average throughput of 40%, which is consistent with the 2004 measurement when considering the amount of light lost to the primary and secondary mirror surfaces and optics internal to the WFS.

For the Lick dye laser, the relatively long dark time between pulses (~91 μs) makes it only necessary to simulate a single cycle. The ~38 μs dark time between pulses in the Keck laser is near the critical timescale where the sodium atom excitation levels accumulate from pulse to pulse, hence a single pulse and a train of 5 pulses were modeled and compared. The return from the 5 pulse simulation was only ~8% less than for the single. This small change reinforces the above conclusion that the rethermalization time is near 50 μs. A spot size of 0.7 m FWHM was assumed for both, and other parameters based on location, such as different altitudes and magnetic field direction and strength, were included in the model.

The simulations indicate these pulsed lasers should be producing, at the location of the telescope, 3.9 and 4.5 x10^6 photons/s/m^2, for Lick and Keck respectively, which is ~3.5 times greater than actual measurements. These predictions are for the mean seasonal expected Na column density of 4 x10^{13} atoms/m^2, used for all previous modeling results. Making adjustments to not completely constrained parameters such as spot size, launched power, bandwidth, and atmospheric transmission, can somewhat ameliorate this disagreement. For example, in the case of the Shane laser, the estimate can be reduced 20% by changing the modeled spot size to 0.6 m FWHM and increasing the bandwidth to 2.2 GHz. This same reduction is also found from increasing the spot size to 1.0 m FWHM, setting the bandwidth 2.2 GHz, and decreasing the atmospheric transmission to 85% (the default value is 89%). The target bandwidth for this laser was 1.5 GHz, but measurements from the observatory indicate the FWHM is closer to 2.2 GHz, and the actual shape is closer to a step function than a Gaussian, which has not been included in the model.

Because the return flux at the telescope scales linearly with the Na column density, this parameter can be used as a gauge in determining how accurately a numerical model reproduces real systems. Results of Lidar measurements indicate the expected median annual density is 3 – 4 x10^{13} atoms/m^2, although sporadic layers may have concentrations up to 10 times greater[12,13]. Applying this to the best prediction for the Lick dye laser (where the return flux is 3.12 x10^6

photons/s/m^2, taking into account the 20% reduction discussed in the previous paragraph) would indicate that the mean Na column density above Mt. Hamilton is 1.5 x10^{13} atoms/m^2. In Figure 5 data from the this laser taken between 2006 and 2010 are plotted, with the right-hand axis exhibiting the implied amount of Na based on our current level of modeling. The expected seasonal variation is evident in these measurements.

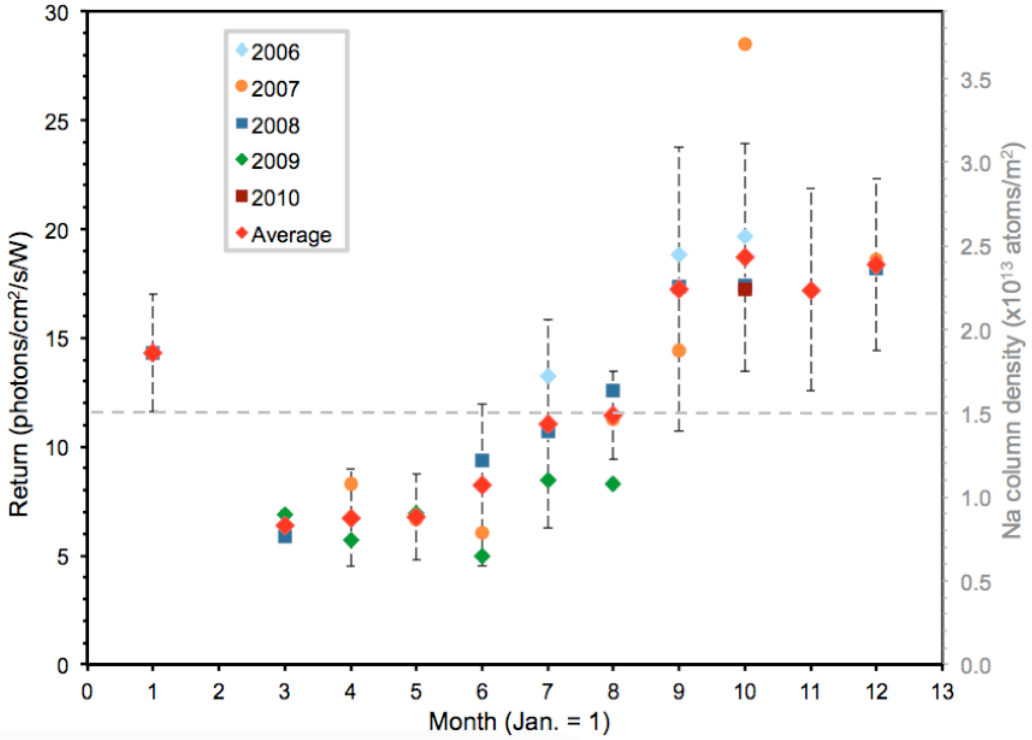

Figure 5. Data from the dye laser on the Shane telescope show the expected seasonal variability. The right axis shows implied values of Na column density based on our current level of modeling with LGSBloch. The horizontal dashed line indicates the predicted average column density based on the measured average return of 1.13 x10^6 photons/s/m^2, or equivalently 11.3 photons/cm^2/s/W. These are considerably lower than expected, implying the need for simulation with greater detail.

We consider this inconsistency between the model and actual measurements from these short pulse dye lasers to signal a need for inclusion of greater detail in the simulations. The LGSBloch package in its current form successfully predicts the return measurements seen from narrow bandwidth CW LGS (i.e. the 50 Watt FASOR at the Starfire Optical Range), and reproduced the relative factor of ~3 reduction in return flux seen at the Shane telescope when the spectrum broadening phase modulator was switched off (due to increased saturation). It seems plausible that the significantly higher peak powers during a short pulse (~5000 Watts for the Shane LGS) make it necessary to account for a realistic speckled irradiance pattern in the mesosphere, instead of the simplified Gaussian profile. Additional factors to investigate include unknown power losses due to off wavelength light and projection optics, and the effects of a broad top hat shaped spectrum. However, because the discrepancy is constant for the two observatories, future considerations must investigate the relevant influences present at both.

Further experimental confirmation of LGSBloch simulations will soon be provided by the recently commissioned European Southern Observatory Wendelstein transportable 20W LGS unit[14]. This system is designed to do systematic field studies of LGS return flux vs. laser parameters. Its capabilities include adjustment of the output polarization state, variable line width between ~5–25 MHz, adjustable repumping up to 30%, and pulse modes with amplitude modulation frequencies between 1 and 700 kHz.

5. DISCUSSION

The use of numerical models has made it possible to investigate the effects of different parameters involved in LGS creation. This allows optimization of the format and estimation of the photon return prior to installing the laser at the telescope. This tool has determined some basic guidelines as to the most efficient way to couple the laser light to the Na atoms. These include using narrow bandwidth, circularly polarized light, with ~10% of the power tuned to the D_2b transition.

These simulations also show that photon returns close to those from CW lasers can be achieved with long pulse formats. Pulses enable Raleigh blacking and fratricide avoidance strategies to be implemented. Thus far we have discussed results for a 10 Watt laser operating with 10% and 20% duty cycles, and pulse durations ranging from 200 ns to 60 μs. For the case of 10% repumping, the 20% duty cycle pulses result in ~20% greater return and have a slight maximum when around 30 μs in duration. This maximal value is within 10% of what is expected from a 10 Watt CW laser operating in the same conditions.

Longer duty cycles were also investigated for this laser, keeping all other parameters the same as in Section 3. Three pulse cycles were simulated for the cases of 50% and 75% duty cycles, resulting in predicted returns of 12.5 and 12.9 photons/s/m^2, respectively, which are clearly asymptoting to the predicted CW return value.

Another interesting avenue these simulations enable us to explore is the possible benefits of uplink control, where the laser light is reflected off a deformable mirror prior to projection. This allows manipulation of the wavefront in order to correct for aberrations due to atmospheric turbulence and imperfections in the projection optics. In Figure 6, return flux at the telescope is plotted versus r_0 (Fried's parameter), which is equivalent to varying spot sizes in the mesosphere. These simulations are for a 10 Watt CW zenith pointing laser operating at Mt. Hamilton. Since the return is greater for larger spots (smaller r_0), the implication is uplink control can be used to optimize between this enhancement and the corresponding reduction in WFS signal-to-noise, which declines as the square of the spot size (equation 1 in reference 7). In future work, we will investigate using uplink techniques to manipulate the irradiance profile as well as the spot size, in order to maximize the area in the mesosphere irradiated at the most efficient levels (as mentioned in Section 3). This will involve modeling a beam profile with a shape more like a top hat, in contrast to the Gaussian profiles used thus far.

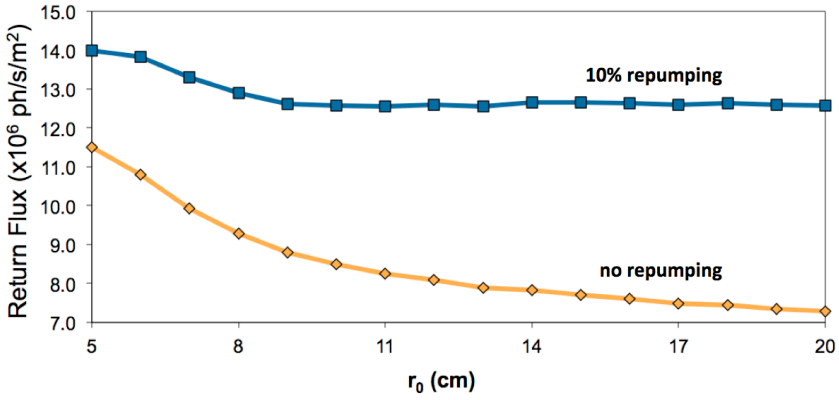

Figure 6. The return increases in poor seeing conditions (i.e. small r_0) due to the larger spot size produced in the mesosphere, allowing more atoms to interact with the light. This effect is less substantial when using repumping. Uplink control could optimize between this enhancement and the reduction in WFS signal-to-noise due to the larger spot.

REFERENCES

[1] T. H. Jeys, "Development of a mesospheric sodium laser beacon for atmospheric adaptive optics," Lincoln Laboratory Journal 4, 133–150 (1991).

[2] W. Happer, G. J. MacDonald, C. E. Max, and F. J. Dyson, "Atmospheric-turbulence compensation by resonant optical backscattering from the sodium layer in the upper atmosphere," J. Opt. Soc. Am. A 11, 263–276 (1994).
[3] R. Holzlöhner, S. M. Rochester, D. Bonaccini Calia, D. Budker, J. M. Higbie, and W. Hackenberg, "Optimization of cw sodium laser guide star efficiency," Astron. Astrophys. 510, A20+ (2010).
[4] Available at http://budker.berkeley.edu/ADM/.
[5] P. W. Milonni, R. Q. Fugate, and J. M. Telle, "Analysis of measured photon returns from sodium beacons," J. Opt. Soc. Am. A 15, 217–233 (1998).
[6] A. Corney, *Atomic and Laser Spectroscopy* (Clarendon, Oxford, 2006).
[7] D. Gavel, H. Friedman, "Measurements of the Lick Observatory sodium laser guide star," Proc. SPIE 3353, 0277-786, (1998).
[8] C. Denman, J. Drummond, M. Eickhoff, R. Fugate, P. Hillman, S. Novotny, J. Telle, "Characteristics of sodium guidestars created by the 50-watt FASOR and first closed-loop AO results at the Starfire Optical Range," Proc. SPIE 6272 (2006).
[9] J. Dawson, A. Drobshoff, R. Beach, M. Messerly, S. Payne, A. Brown, D. Pennington, D. Bamford, S. Sharpe, and D. Cook, "Multi-watt 589nm fiber laser source," Proc. SPIE 6102 (2006).
[10] D. Le Mignant, R. Campbell, A. Boucheza, J. Chin, E. Chock, A. Conrad, M. van Dam, S. Doyle, R. Goodrich, E. Johansson, R. Lafon, J. Lyke, C. Melcher, R. Mouser, D. Summers, C. Wilburn and P. Wizinowich, "LGS AO operations at the W. M. Keck Observatory," Proc. SPIE 6270 (2006).
[11] http://www.eso.org/sci/observing/tools/standards/spectra/stanlis.html
[12] N. Moussaoui, B. R. Clemesha, R. Holzlöhner, D. M. Simonich, D. Bonaccini Calia, W. Hackenberg, and P. P. Batista, "Statistics of the sodium layer parameters and its impact on AO sodium LGS characteristics," Astron. Astrophys. 511, A31 (2010).
[13] Xiong, H., Gardner, C.S., and Liu, A.Z., "Seasonal and nocturnal variations of the mesospheric sodium layer at Starfire Optical Range, New Mexico", Chin. J. of Geophys. 46, pp. 432–437 (2003).
[14] D. Bonaccini Calia, R. Holzlöhner, I. Guidolin, F. Pedichini, M. Centrone, T. Kasper, G. Lombardi, W. Forth, S. Lewis, T. Pfrommer, and W. Hackenberg, "ELT LGS-AO: Optimizing the LGS Return Flux," Proc. AO4ELT2 (2010).